CONTROL STRATEGY OF SWITCHING REGULATORS FOR PHOTO VOLTAIC POWER APPLICATIONS

SARASWATHI PALEM[1] NAGARJUNA KADIRI[2]

[1]*Pg scholar, Department of EEE (POWER SYSTEMS), Avanthi Institute of Engineering & Technology, Hyderabad, TS, India*

[2]*Assistant Professor, Department of EEE, Avanthi Institute of Engineering & Technology, Hyderabad, TS, India*

ABSTRACT

Usually accepted that input voltage source of a switch-mode power supply is constant or shows insignificant small variations. Despite everything, the last assumption is not any more valid when an PV is utilized as input source. A PV is described by low and unregulated DC output voltage, moreover, this voltage diminishes in a non-linear form when the demanded current increments; from now on, an appropriate controller is required to adapt the previously mentioned issues. In this investigation, a normal current-mode controller is planned utilizing a joined model for an energy unit PV and a boost converter; besides, a determination method for controller picks up guaranteeing system stability, o/p voltage regulation is produced. The proposed energy system utilizes an energy component power module and a boost converter conveying a power of 900 W. Simulation results affirm the proposed controller execution for o/p voltage regulation by means of closed loop gain estimations and step load changes. What's more, a correlation amongst open-and closed loop estimations is made, where the controller robustness is tried for vast load varieties and PV stack o/p voltage changes also.

KEY TERMS: PV, Boost converter, Current-mode controller

1. INTRODUCTION

Photovoltaics offer buyers the capacity to produce power in a spotless, calm and dependable way. Photovoltaic systems are contained photovoltaic cells, devices that proselyte light energy straightforwardly into power. Since the wellspring of light is normally the sun, they are regularly called solar cells. The word photovoltaic originates from "photograph," meaning light, and "voltaic," which alludes to creating power. Along these lines, the photovoltaic procedure is "delivering power straightforwardly from daylight." Photovoltaics are regularly alluded to as PV. PV cells convert daylight straightforwardly into power without making any air or water contamination. PV cells are made of somewhere around two layers of semiconductor material. One layer has a positive charge, the other negative.

At the point when light enters the cell, some of photons from light are consumed by the semiconductor molecules, liberating electrons from cell's negative layer to course through an outer circuit and once again into the positive layer. This stream of electrons produces electric current. To expand their utility, dozens of individual PV cells are interconnected together in a fixed, weatherproof bundle called a module. At the point when two modules are wired together in series, their voltage is multiplied while the present remains constant. At the point when two modules are wired in parallel, their current is multiplied while the voltage remains constant. To accomplish the coveted voltage and current, modules are wired in series and parallel into what is known as a PV exhibit. The adaptability of secluded PV system enables planners to make solar power systems that can meet a wide assortment of electrical needs, regardless of how extensive or little. A grid-associated PV system will require an utility interactive DC to AC inverter. This gadget will change over the immediate current (DC) power delivered by the PV exhibit into rotating current (AC) power normally required for loads, for example, radios, TVs and iceboxes. For an off-grid PV system, shoppers ought to consider whether they need to apply the immediate current (DC) from PV's or convert the power into substituting current (AC). Machines and lights for AC are adequate more typical and are by and large less expensive, yet the change of DC power into AC can devour up to 20 percent of all the power created by the PV system.

2. PROPOSED SYSTEM

A PV is warm - based electrical energy source that creates low and unregulated DC voltage, where the output voltage diminishes in a non-linear mold when the requested current increments. The stack output voltage terminals are associated with a DC/DC power converter to at long last give a voltage required to sustain either a DC or an AC load. In accompanying, a general numerical portrayal

catching correctly the coupling between the PV and a DC/DC boost converter is appeared in detail.

2.1 PV Static Properties

A few articulations have been proposed in open writing to anticipate the warmth and warm dynamical conduct of PV. Be that as it may, with the end goal of this work, a reasonable and simple to-deal with PV articulation incorporating electric properties perfect with power change is utilized. For example, a PV static articulation for o/p voltage which depends on the output present and physical parameters is given in [13]where v f is PV output voltage, if is the pv-cell stack current and E O is the open-circuit voltage.

$$V_f(i_f) = \frac{E_O}{1+(i_f/I_h)^{\delta}} \ldots\ldots\ldots 1$$

The parameters δ and I_h rely upon the earth moistness conditions and stack temperature. These parameters together with E_O are required to be registered for a given pv-cell stack. Sadly, this diode respects an undesired power dissemination, which results in a decrease of usable output power to around 1 kW.

Remark 1: The articulation that speaks to the static properties of pv (1) was taken from [13]; in any case, a system is required to get (from accessible estimated information) the parameters δ and I_h. In accompanying, a clarification about the calculation of parameters E_O, δ and I_h is given. An arrangement of N discrete trial tests (i_{fexp}(k), v_{fexp}(k)) with k = 1, 2, 3, … , N, comparing to the stack o/pcurrent,voltage are required. For this situation, the examples are portrayed in hovers in Fig. 1a. See that such examples are gotten by expanding if from 0 to 43 A (diminishing a resistive load). Note that there is no load associated with the stack at the specific first example; accordingly, the open-circuit voltage is E_O = v_{fexp}(1) when i_{fexp}(1) = 0 A. Presently, the articulation (1) perhaps changed as

$$\left(\frac{i_f}{I_h}\right)^{\delta} = \frac{E_O}{v_f} - 1 \quad \ldots\ldots\ldots\ldots\ldots\ldots 2$$

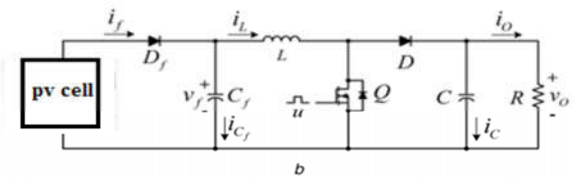

Fig1: PV-cell stack/boost converter system PV-cell stack/boost converter system

and recalling some basic logarithm properties, (2) perhaps expressed as

$$\delta log i_f - \delta log I_h = log\left(\frac{E_O}{v_f} - 1\right) \ldots\ldots\ldots\ldots\ldots 3$$

Expecting that (3) holds for every recorded example (i_{fexp} (k), v_{fexp} (k)) with E known, at that point (3) has the shape where

$$a_1 x + a_0 = y, \ldots\ldots 4$$
$$a_1 = \delta,$$
$$x = \log i_f$$
$$a_0 = -\delta log I_h$$
$$y = log\left(\frac{E_0}{v_r} - 1\right) \ldots\ldots\ldots 5$$

Along these lines, the constants a1 and a0 are required to be found so as to figure δ and I_h. At long last, utilizing the outstanding linear slightest square information fitting [24], the parameters δ and I_h perhaps acquired from accompanying calculations (all entireties are of frame $\sum k_N$= 1):
Which yield to

$$\delta = \frac{N\sum x_k y_k - \sum x_k \sum y_k}{N\sum x_k^2 - (\sum x_k)^2} = 0.64$$
$$I_h = log^{-1}\left(\frac{a_0}{\delta}\right) = 82.86 \ldots\ldots\ldots\ldots\ldots\ldots 7$$

for N = 22 tests and EO = 41.7 V. An examination between trial information and the articulation in (1) is given in Fig. 1a, which affirms the precision of portrayed strategy. Furthermore, this static model (1) is nonstop for a vast scope of currents, including no present and greatest current.

2.2 Overall mathematical representation

The proposed physical usage of pv-cell stack/boost converter system is appeared in Fig. 1b, where Q is the active switch [metal– oxide–semiconductor field-impact transistor (MOSFET)], the obligation cycle, D the diode, L the filter inductor, C the filter capacitor and R the load opposition. Along these lines, i_f, iC_f, i_L, iC and I O are the normal pv-cell, coupling capacitor, inductor, capacitor and o/p currents, individually. At last, the normal pv-cell voltage and o/p (capacitor) voltage are v_f and v_O, individually. In this work, it is accepted that boost converter works in ceaseless conduction mode, i.e. the inductor current never rots to zero [25]. The dynamic conduct of numerous classes of power circuits are analyzed utilizing the idea of normal models, which perhaps controlled utilizing standard circuit strategies. In this sense, utilizing Kirchhoff laws when Q is ON/OFF and the current if from (2), the normal (swell free) ceaseless non-linear model is gotten as

$$v_f = \frac{1}{c_f}\left(I_h\left(\frac{E_O}{v_f}-1\right)^{\frac{1}{\delta}} - i_L\right),$$

$$i_L = \frac{1}{L}(v_f - (1-u)v_o),$$
$$v_o = \frac{1}{C}\left((1-u)i_L - \frac{V_O}{R}\right)\text{.....8}$$

where the state vector is $[v_f, i_L, v_O]^T \in \mathbb{R}^3$ and the info u ∈ (0 1). The non-linear differential conditions in (8) are said to be bilinear, since the info flag u is increasing the state factors v_O and i_L specifically. See that limitations vf∈ℝ+ and iL∈ℝ+ keep away from uncertainty in primary differential condition and guarantees the constant conduction mode operation.

Remark 2:

A connection capacitor is associated in middle of pv-cell stack and the boost converter, meanwhile [27] utilizes a series inductor for a similar errand. In steady state, the normal o/p voltage VO is more prominent than the info Vf, additionally the inductor current IL equivalents to the pv-cell current I f; accordingly, the ostensible working states of (8) are observed to be

$$V_0 = \frac{V_f}{1-U}$$
$$I_L = \frac{V_0}{R(1-U)} = I_h(\frac{E_0}{V_f} - 1)^{1/\delta}\text{.....9}$$

Once the ostensible o/p voltage VO is characterized, the subsequent PV voltage Vfperhaps processed from numerical arrangement of Note that perfect segments and zero voltage losses are expected in (8)– (10); subsequently, the numerical results may contrast from those practically speaking. Moreover, in steady-state CCM operation, the voltage and current swells for boost converter because of switching activity perhaps processed by

$$\Delta V_O = \frac{I_O U}{C f_s}, \Delta I_L = \text{.....10}$$

Moreover, to guarantee CCM, the inductor esteem must be chosen as

$$L > \frac{U(1-U)^2 U}{2 f_s}\text{.....11}$$

respects the linear normal little flag show for general system as

$$\begin{bmatrix} v_f \\ i_L \\ v_o \end{bmatrix} = \begin{bmatrix} -\frac{1}{C_f k} & -\frac{1}{C_f} & 0 \\ \frac{1}{L} & 0 & -\frac{1-U}{L} \\ 0 & \frac{1-U}{C} & -\frac{1}{RC} \end{bmatrix} \begin{bmatrix} v_f \\ i_L \\ V_O \end{bmatrix} + \begin{bmatrix} 0 \\ \frac{V_0}{L} \\ \frac{I_L}{C} \end{bmatrix} u \text{ .....12}$$

where the new state vector is $[v_f, i_L, v_O]^T \in \mathbb{R}^3$ and

$$k = \frac{E_O \delta I_h^{\delta} I_f^{\delta-1}}{(I_h^{\delta} + I_F^{\delta})^2}$$

.....13

The subsequent model (13) consolidates two subsystems dynamics and has just a single information u~ ∈ℝ. This linear time-invariant model depicts roughly the conduct of pv-cell stack/boost converter system for frequencies up to half of switching frequency f s. Besides, it tending utilized for examination and controller plan of switching controllers.

3. PROPOSED AVERAGE CURRENT-MODE CONTROLLER

Normal CMC is a helpful system for facilitating the outline and enhancing the dynamic execution of switch-mode converters. Here, an approach to legitimately choose the controller gains for steadiness and execution reasons for existing is given. Since the normal inductor current is utilized for o/p voltage regulation, a quicker reaction is gotten when step changes are connected to the load. Moreover, detecting the inductor current can likewise be utilized for counteracting overload current through converter. This control method utilizes a high-gain compensator, a low-pass filter and a PI controller to warrant: (I) that normal inductor current takes after the present reference, and (ii) output voltage regulation.

The upside of this methodology is that any adjustment in info voltage source has a quick impact in controller (quick spread property). The general controller plan technique is a twofold issue: (I) gain determination for present circle, and (ii) gain choice for voltage circle. With a specific end goal to determine the controller articulations, a design for this method is proposed in Fig. 2. As perhaps seen, the normal CMC utilizes current,voltage circles. For present circle, N is the present sensor gain, G(s) a high-gain compensator, F(s) a low-pass filter lastly VP the pinnacle size of slope used to create the control pulses. For voltage circle, H remains for voltage sensor gain, Vref the coveted output voltage and K(s) the exchange work comparing to the PI controller, which produces the present reference I_{ref}.

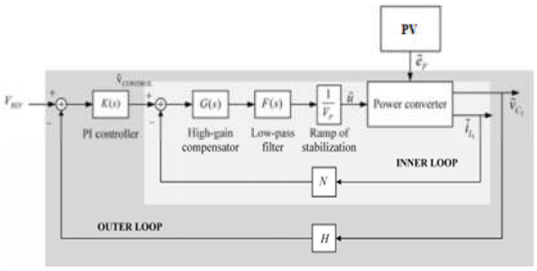

Fig2: Average CMC scheme for a switching regulator

Remark 3:

The control conspire proposed has two control circles for o/p voltage regulation also, yet the high-gain compensator and the low-pass filter are coordinated to voltage circle, meanwhile the present circle is actualized by a hysteresis controller. For robust steadiness of each circle, the accompanying prerequisites must be fulfilled:

i. for relative soundness, the incline at or close traverse frequency must be not more than −20 dB/dec;

ii. to enhance steady-state exactness, the gain at low frequencies ought to be high;

iii. for robust soundness, suitable gain and stage edges are required. In accompanying, simple to-utilize formulae are given to guarantee fitting circle picks up attributes of shut circles. The poles and zeros for proposed controller are set chiefly from working switching frequency of converter.

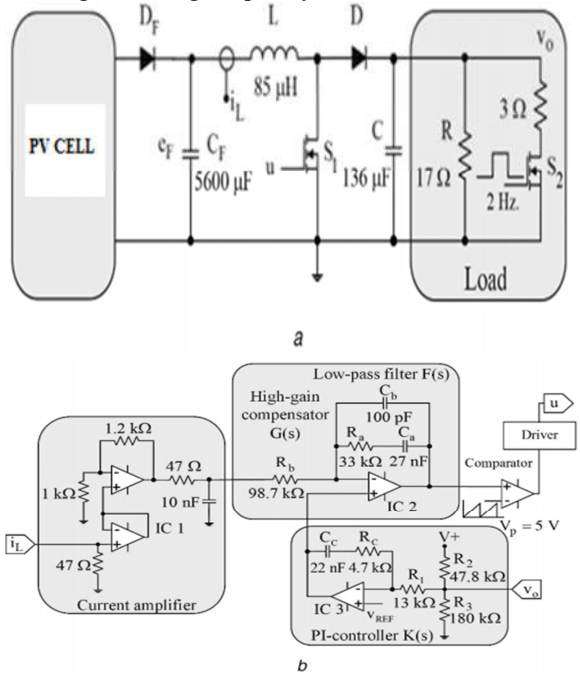

Fig3: Switching regulator (a) Combined photovotaic-cell stack/boost converter, (b) Average current-mode controller

• The zero ω Z of high-gain compensator ought to be set somewhere around 10 years underneath of half of PWM switching frequency, f s/2. Essentially, the zero is controlled by the relationship

$$\omega_Z = \frac{1}{R_a C_a} \text{.....14}$$

where R an and Ca are the obstruction and capacitance relating to the present circle control circuit.

• The shaft ωPof low-pass filter, then again, ought to be put either at f s/2 or above. Utilizing the circuitry in Fig. 4, the post is controlled by

$$w_P = \frac{C_a C_a}{R_a C_a C_a} \text{.....15}$$

where C b is the capacitor related to the present circle circuit too.

• The compensator gain is processed by

$$G_p = \frac{R_a}{R_b} \text{.....16}$$

.

where the opposition esteems must be carefully chosen with the end goal that

$$Gp < \frac{5(1-U)^2 R}{NV_0} \text{.....17}$$

Voltage loop

The external circle ought to be intended to give an appropriate steady state revision of o/p voltage and perhaps actualized utilizing a PI controller. The o/p of this circle is the present reference

$$Iref = K_C\left(1 + \left(\frac{1}{T_i S}\right)\right)(V_{ref} - Hv_o) \text{.....18}$$

where K C is the relative gain, Ti is the indispensable time and Vref is the reference o/p voltage. For this situation, the choice criteria ought to take after:

• The proportional gain KP = RC/R1 is selected such that

$$K_P < \frac{10(1-U)}{HV_O} \text{.....19}$$

where the voltage divider is

$$H = \frac{R_1 I I R_3}{R_1 I I R_3 + R_2} \text{.....20}$$

• Finally, the integral time is computed from

$$T_i = R_C C_C \text{.....21}$$

where R C and CC are the opposition and capacitance estimations of PI controller circuit, which must be chosen with the end goal that 1/Ti is put no less than multi decade beneath f s.

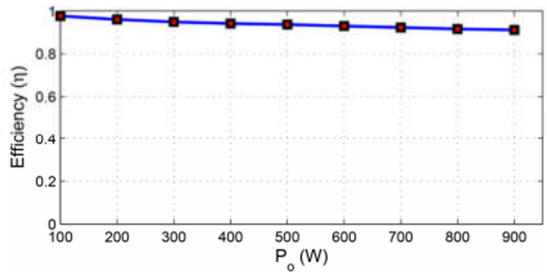

Fig4: Experimental efficiency (η) of power converter. The converter effectiveness (η = Po/Pi, where Po is the o/p power and Pi is the information power of converter) is appeared in Fig. 4, as perhaps seen, the effectiveness lessens when the o/p power is expanded.

Remark 4:

Rather than VMC, here an internal circle is included. This enhances altogether the transient execution of controller, since the exchange work v~ O/u~ of a boost converter has a correct half-plane zero, and a solitary voltage circle may not bargain appropriately with this issue.

SIMULATION RESULTS

A pv-cell stack/boost converter and the relating controller (16) have been actualized in research facility as demonstrated Fig. 4. The converter parameters are given in Table 1. The boost converter ostensible obligation cycle U is set to 0.56, giving an output voltage of V O = 48 V, nourishing an ostensible resistive load of R = 2.56 Ω. The aggregate o/p power is around 900 W, which requires an arrived at the midpoint of fuel utilization of 12.2 standard liter for each moment. Besides, the switching frequency is set to 100 kHz. The pinnacle greatness of incline VP is 5 V and the voltage sensor gain H is 0.20. The parameters of controller are chosen seriate the above criteria: f Z = ωZ/2π = 178.62 Hz, GP = 0.33, f P = ωP/2π = 48.4 kHz, KP = 0.36 and Ti = 0.103 ms. Open-and shut circle test tests were performed considering step changes in load opposition through switch S2. These varieties go from 2.56 to 17 Ω; that is from full to 10% of load at a frequency of 2 Hz.

Open-loop test

The test reaction of exchange work i~L/u~ is appeared in Fig. 5a, while the trial reaction of exchange work ~v O/u~ is appeared in Fig. 5b. These exchange capacities were estimated at ostensible load utilizing the Frequency Response Analyser 300 from AP Instruments, Inc. Both frequency reactions were gotten in open circle, moreover, it is obvious from plots that full pinnacles happen around 1.1 kHz.

The simulation open-loop time response of system is shown in Fig. 6a. It is noticeable that experimental results are close enough to the theoretical relation given in (9). Using the MOSFET S 2 (trigger voltage Vg), step changes of 2 Hz are applied to the o/p load which ranges from 2.56 to 17 Ω. The resulting o/p voltage VO is shown in Fig. 6b, which changes for about 33 V. On the other hand, Fig. 6c shows the step changes on the pvcell side. As perhaps seen, the pvcell stack o/p voltage ranges from 23 to 33 V and the demanded current changes from about 9 to30A

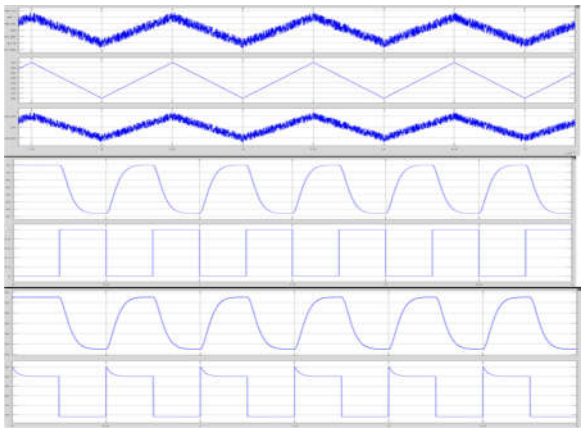

Fig5. Experimental results in open-loop response for step changes in load between 2.56 and 17 ohm(a) (top to bottom) o/p voltage V_o(20 V/div),inductor current i_L (25 A/div) and PV cell voltage v_f(20 V/div) (time:10ms/div),(b)(from top to bottom) output voltage v_O(20 V/ div) and gate voltage Vg of MOSFET S2 (20 V/div)(time: 200 ms/div), (c)(from top to bottom) output voltage of PV-cell stack v_f(20 V/ div) and output current of PV cell stack I f(10A/div)(time: 200 ms/div)

Closed-loop test

The switching regulator operating condition corresponding to 48 V o/p voltages at nominal load (no load changes) is shown in Fig. a. At this operating condition, the pv-cell stack is delivering a voltage of 24 V. When o/p load changes are introduced, the resulting load voltage remains at 48 V as shown in Fig. 26b, where it is clear the switching regulator is robust under large load variations. As consequence of these changes, the pv-cell stack voltage changes between 26 and 38 V. The demanded current ranges from 4 to 27 A, as is shown in Fig. 6c. There are significant differences between current, voltage levels in Figs2c and.25c, respectively. This is due to stored energy in capacitor CF that helps to compensate the changes in demanded energy for closed-loop response. Note that PV cell current in open loop case (Fig. 5c) presents a 5 A overshoot, meanwhile in closed-loop case (Fig.6c), the current

does not present any overshoot; therefore, the life cycle of PV is not overwhelmed. The current ripple is shown in Fig. 6d, which is small (1.2 A peak to peak) due to the capacitor CF.

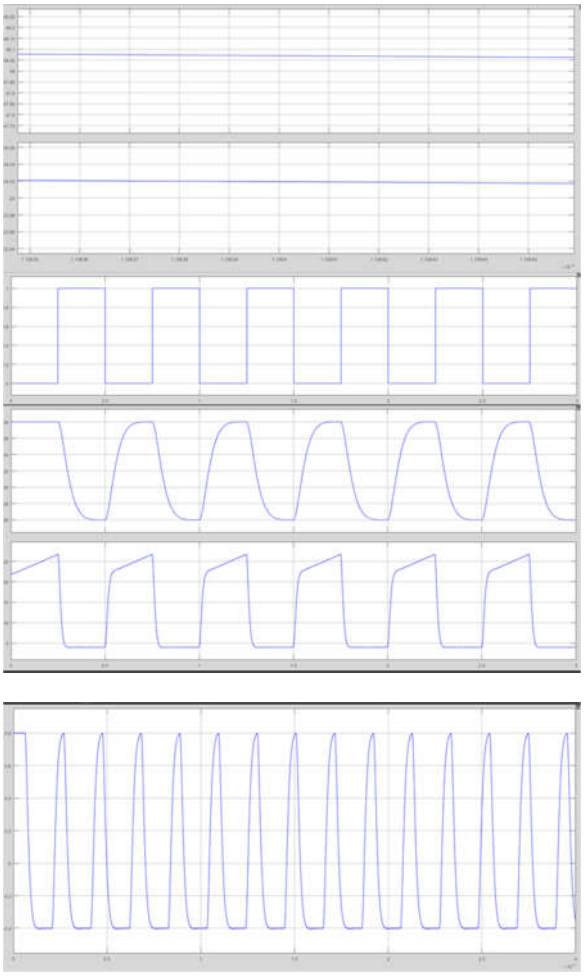

Fig 6: Closed-loop response (a) Response at nominal load ((b) Response to step changes in load (c) Response to step changes in load between 2.56 and 17 Ω: (from top to bottom) pv-cell voltage vf (20 V/div), and o/p current of pv-cell stack if (10 A/div) (time: 200 ms/div), (d) Output current ripple of pv cell stack i f (1 A/div) (time: 10 µs/div)

CONCLUSIONS

This report manages the output voltage regulation of a PV cell stack/boost converter system. The proposed control methodology depends all things considered CMC where two circles are executed, in particular the internal circle where the inductor current is sustained back utilizing a high gain compensator and a low-pass filter, and the external circle where the output voltage is encouraged back through a PI controller for steady-state mistake regulation. The determination technique for controller parameters is expressly point by point. The criteria given inside guarantee system solidness and output voltage regulation. The shafts and zeros for controller are set fundamentally from working switching frequency of converter. Furthermore, because of high-gain compensator of inward circle, the converter execution is less delicate to parameter vulnerabilities and varieties of PV cell stack voltage. This control procedure was actualized utilizing ease operational speakers, reasonable for business applications. At last, trial results utilizing a 900 W boost converter model show great robustness to expansive minor departure from load.

REFERENCES

[1] Carrasco, J.M., Garcia, L., Bialasiewiez, J.T., et al.: 'Power-electronic system for the grid integration of renewable energy sources', IEEE Trans. Ind. Electron., 2006, 53, (4), pp. 1002–1016

[2] Benson, Ch.L., Magee, Ch.L.: 'On improvement rates for renewable energy technologies: solar PV, wind, capacitors, and batteries', J. Renew. Energy, 2014, 68, pp. 745–751

[3] Shen, J.-M., Joul, H.-L., Wu, J.-C.: 'Transformerless three-port grid connected power converter for distribution power generation system with dual renewable energy sources', IET Power Electron., 2012, 5, (1), pp. 501–509

[4] Jakhar, H., Soni, M.S., Gakkhar, N.: 'Historical and recent development of concentrating photovoltaic cooling technologies', Renew. Sustain. Energy Rev., 2016, 60, pp. 41–59

[5] Bahceci, S., Fedakar, S., Yalcinoz, T.: 'Examination of the grid-connected polymer electrolyte membrane PV's electrical behaviour and control', IET Renew. Power Gener., 2016, 10, (3), pp. 388–398

[6] Rahmal, S.A., Varmal, R.K., Vanderheide, T.: 'Generalised model of a photovoltaic panel', IET Renew. Power Gener., 2014, 8, (3), pp. 217–229

[7] Li, Q., Chen, W., Liu, Z., et al.: 'Active control strategy based on vector proportion integration controller for proton exchange membrane PV grid-connected system', IET Renew. Power Gener., 2015, 9, (8), pp. 991–999

[8] Thounthong, P., Davat, B., Rael, S., et al.: 'PV high-power applications', IEEE Ind. Electron. Mag., 2009, 3, pp. 32–46

[9] Kabalo, M., Pairel, D., Blunier, B., et al.: 'Experimental evaluation of four phase floating interleaved boost converter design and control for PV applications', IET Power Electron., 2013, 6, (2), pp. 215–226

[10] Leel, J.-G., Choe, S.-Y., Ahn, J.-W., et al.: 'Modelling and simulation of a polymer electrolyte membrane PV system with a PWM dc/dc converter

for stationary applications', IET Power Electron., 2008, 1, (3), pp. 305–317

[11] Thounthong, P., Davat, B.: 'Study of a multi-phase interleaved step-up converter for PV applications', Energy Convers. Manage., 2010, 51, pp. 826–832

[12] Naik, M.V., Samuel, P.: 'Analysis of ripple current, power losses and high efficiency of dc–dc converters for PV power generating systems', Renew. Sustain. Energy Rev., 2016, 59, pp. 1080–1088

[13] Shahin, A., Hinaje, M., Martin, J.-P., et al.: 'High voltage ratio dc–dc converter for fuel-cell applications', IEEE Trans. Ind. Electron., 2010, 57, (12), pp. 3944–3955

[14] Hajizade, A., Golkar, M.A., Feliachi, A.: 'Voltage control and active power management of hybrid fuel-cell/energy-storage power conversion system under unbalanced voltage sag conditions', IEEE Trans. Energy Convers., 2010, 25, (4), pp. 1195–1208

[15] Vazquez-Oviedo, E.I., Ortiz-Lopez, M.G., Diaz-Saldierna, L.H., et al.: 'Modeling study of a combined fuel-cell stack/switch mode dc–dc converter', J. PV Sci. Technol., 2014, 11, pp. 1–5

[16] Leyva-Ramos, J., Lopez-Cruz, J.M., Ortiz-Lopez, M.G., et al.: 'Switching regulator using a high step-up voltage converter for fuel-cell modules', IET Power Electron., 2013, 6, (8), pp. 1626–1633

[17] Saadi, R., Kraa, O., Ayad, M.-Y., et al.: 'Dual loop controllers using PI, sliding mode and flatness controls applied to low voltage converters for PV applications', Int. J. Hydrog. Energy, 2016, 41, (42), pp. 19154–19163.

AUTHORS PROFILE

SARASWATHI PALEM Completed her Bachelor of technology(B.Tech) from Avanthi Institute of Engineering and Technology in the year 2015 and pursuing Master of Technology(M.tech) From Avanthi Institute of Engineering and Technology for the academic year 2016-2018

Nagarjuna Kadiri completed his Bachelor of Technology (B.Tech.) from Prakasam Engineering college in the year 2009 and Master of Technology (M.Tech.) from QIS institute of engineering. Presently, he is pursuing Ph.D (part time) from Sathyabama Institute of Science and Technology (Deemed to be University) Chennai. Right now, he is working in Avanthi Institute of Engineering & Technology and he has around 7 years of teaching experience. His research interest includes Power Electronics, Renewable energy sources, electrical drives etc.